

1,7-homo hydrogen shift products from **2** at 100 °C in solution is 0.9:1.0 with **4** being the major 1,7-shift product at low conversions.<sup>4</sup>

A significant difference between the previously reported product distribution from flow system pyrolysis of **1** and these results is the observation of only small amounts of **2** in the gas-phase, static pyrolysis of **1**. The present observations are reasonable given the kinetics for conversion of **2**. For sequential first-order reactions the mole fraction of **2** calculated to be present over the time range investigated at 209.0 °C is 0.002–0.004. The observed values are  $0.005 \pm 0.002$ . This agreement lends credibility to the suggestion<sup>1</sup> that **2** is, indeed, along the reaction pathway. We have found that **1** and related hydrocarbons, like  $\alpha$ -pinene,<sup>8c</sup> are very sensitive to wall catalysis, and surface catalysis of the rearrangement of **1** may have been responsible for the flow system product distribution.

The *syn*-7-(trideuteriomethyl) derivative of **1**, **1-d<sub>3</sub>**,<sup>1</sup> was also pyrolyzed in the static reactor at 209.0 °C. The GC peak corresponding to **2** on two different columns increased by a factor of ~4 at both 15% and 29% conversion. The ratio of 1,5- to 1,7-hydrogen shift products was not affected by the deuterium. In addition, the high-field <sup>2</sup>H NMR of the reaction mixture revealed a 2:1 ratio of deuterium on the exo methylenes of **3–6** relative to the methyls at both 25% and 45% reaction. Since most of **2** is converted to **3–6** under these conditions and since the hydrogen shifts in **2** have been shown to be stereospecific,<sup>1</sup> this corresponds to 75% inversion and 25% retention in the conversion of **1** to **2**. There was no scrambling (*syn*–*anti* isomerization) in **1-d<sub>3</sub>**. From the kinetics of loss of **1** it was also possible to determine  $k_1^H/k_1^{D_3} = 1.26 \pm 0.05$  at 209.0°.

The factor of 4 increase in the amount of **2** observed upon deuterium substitution is consistent with  $k_2^H/k_2^{D_3} \approx 4$ . This value is reasonable for a primary isotope effect.<sup>5</sup> On the other hand the small kinetic isotope effect in the loss of **1** excludes formation of **3–6** by a process involving C–H bond breaking in the rate-determining step for rearrangement of **1**. However, this small value is consistent with the secondary kinetic isotope effect expected if formation of **2** is the rate-determining step in the loss of **1**.

The activation parameters for disappearance of **1** are consistent with a biradical reaction. The *A* factor is high, and the activation energy is close to the 43 kcal/mol estimated for the dissociation energy of the C-1,C-7 bond using Doering's upwardly revised estimates of C–C bond energies.<sup>6</sup> The major stereochemical path is clearly opposite to the prediction of the Woodward–Hoffmann rules for a concerted suprafacial 1,5-carbon shift, but there is no violation of the Woodward–Hoffmann rules if the reaction is not concerted. We suggest that nonconcerted ring opening occurs in a conrotatory-bevel sense,<sup>7</sup> and this is followed by a least motion closure. These results are similar to those of Klarner,<sup>8a</sup> of Baldwin<sup>8b</sup> on the Berson–Willcott tropilidene circumambulatory 1,5-carbon shift,<sup>9</sup> and of the cleavage of  $\alpha$ -pinene.<sup>8c</sup>

The relatively slow rate of rearrangement of **1** would appear to rule out the intermediacy of bicyclo[4.1.1]octa-2,4-diene in the Grimme–Doering butadienylcyclopropane degenerate rear-

range of bicyclo[5.1.0]octa-2,4-diene ( $t_{1/2} = 0.5$  h vs. 140 h for **1** at 150 °C).<sup>10a</sup> Further, Kirmse found only a small rate effect from 8-methoxy substitution on this diene indicating that cleavage of the C-1,C-8 bond does not occur.<sup>10b</sup> This rearrangement is not observed with **2**, despite the fact that the rate constant for carbon rearrangement of the parent bicyclo[5.1.0]octadiene is comparable to that for the hydrogen shift in **2**. Models suggest that the endocyclic methyl in **2** should sterically destabilize the transition state for the Grimme–Doering rearrangement.

**Acknowledgment.** We thank the NSF and the donors of the Petroleum Research Fund, administered by the American Chemical Society, for generous support of this investigation and Professor Staley for directions to prepare **2**.

**Registry No.** **1**, 62235-10-3; **2**, 57354-42-4; D<sub>2</sub>, 7782-39-0.

(10) (a) Grimme, W.; Doering, W. v. E. *Chem. Ber.* **1973**, *106*, 1765. (b) Kirmse, W.; Kuhr, R.; Murawski, H.-R.; Scheidt, F.; Ullrich, V. *Ibid.* **1980**, *113*, 1272.

### Gas-Phase Infrared Spectroscopy and Recombination Kinetics for Mn(CO)<sub>5</sub> Generated via XeF Laser Photolysis of Mn<sub>2</sub>(CO)<sub>10</sub>

T. A. Seder, Stephen P. Church,<sup>†</sup> and Eric Weitz\*

Department of Chemistry, Northwestern University  
Evanston, Illinois 60201

Received October 11, 1985

There is currently intense interest in the photochemistry of metal carbonyls, in part due to the important role played by coordinatively unsaturated species in a variety of reaction mechanisms. Of particular interest are those species such as Mn<sub>2</sub>(CO)<sub>10</sub> having a metal–metal bond where two distinct types of primary photochemical events can occur; one involving loss of CO without metal–metal bond cleavage and the other involving homolytic cleavage of the Mn–Mn bond. Both processes have been reported in the UV photolysis of solution-phase Mn<sub>2</sub>(CO)<sub>10</sub>.<sup>1,2</sup> In addition, the kinetics of the Mn(CO)<sub>5</sub> recombination reaction and the reaction of Mn<sub>2</sub>(CO)<sub>9</sub> with CO have been measured in solution.<sup>3</sup> Both Mn(CO)<sub>5</sub> and Mn<sub>2</sub>(CO)<sub>9</sub> have also been studied in a matrix environment.<sup>3</sup>

Gas-phase studies are considerably more limited. Freedman and Bersohn have measured the effect of polarized light on the angular distribution of fragments produced via photodissociation of Mn<sub>2</sub>(CO)<sub>10</sub> setting an upper limit of several picoseconds on the excited-state lifetimes.<sup>4</sup> Leopold and Vaida's report of the presence of Mn<sub>2</sub> ion signals in the mass spectrum of the photo-products generated via photolysis of gas-phase Mn<sub>2</sub>(CO)<sub>10</sub> suggests that CO loss is a photochemical pathway in the gas phase.<sup>5</sup>

In this paper we report on the first example of direct detection via transient infrared spectroscopy of the Mn(CO)<sub>5</sub> radical produced via XeF (351 nm) laser photolysis of a gas-phase sample of Mn<sub>2</sub>(CO)<sub>10</sub>. In addition the recombination kinetics of the Mn(CO)<sub>5</sub> radical have been studied, and a rate constant for recombination has been determined. Finally, we are able to make some comments on the nature of the primary photolytic processes

(4) The low *A* factor and small activation energy for rearrangement of **2** are consistent with both hydrogen shifts being concerted as suggested previously.<sup>1</sup>

(5) *anti*-1,5-Bishomocycloheptatriene exhibits a 1° deuterium KIE for the homo-1,5-hydrogen shift of 6.7 at 173 °C. Detty, M. R.; Paquette, L. A. *J. Chem. Soc., Chem. Commun.* **1978**, 365.

(6) Doering, W. v. E. *Proc. Natl. Acad. Sci. U.S.A.* **1981**, *78*, 5279. BDE(3°–4° C–C) = 80 kcal/mol; Pentadienyl radical RE ≈ 19 kcal/mol; RE of diene = 5 kcal/mol. The strain energy for 7,7-dimethylbicyclo[4.1.1]octa-2,4-diene = 36 kcal/mol and biradical intermediate = 13 kcal/mol calculated from a modification by N. L. Allinger's MM2 program (QCPE 345) with MMP1  $\pi$  subroutines (QCPE 318), by J. J. Gajewski and K. E. Gilbert, Indiana University.

(7) Gajewski, J. J. "Hydrocarbon Thermal Isomerizations"; Academic Press: New York, 1981; pp 138–140, 180–182.

(8) (a) Klarner, F.-G. *Angew. Chem., Int. Ed. Engl.* **1974**, *13*, 268. Klarner, F.-G.; Yaslak, S.; Wetter, M. *Chem. Ber.* **1979**, *112*, 1168. Klarner, F.-G.; Brassel, B. *J. Am. Chem. Soc.* **1980**, *102*, 2469. (b) Baldwin, J. E.; Broline, B. *J. Am. Chem. Soc.* **1982**, *104*, 2857. (c) Gajewski, J. J. and Hawkins, C. M. *J. Am. Chem. Soc.*, in press.

(9) Berson, J. A.; Willcott, M. R., III *Rec. Chem. Prog.* **1966**, *27*, 139.

<sup>†</sup> Present address: Max Planck Institut für Strahlenchemie, D-4330 Mülheim a.d. Ruhr, West Germany.

(1) Rothberg, L. J.; Cooper, N. J.; Peters, K. S.; Vaida, V. *J. Am. Chem. Soc.* **1982**, *104*, 3536.

(2) Kobayashi, T.; Yasufuku, K.; Iwai, J.; Yesaka, H.; Noda, H.; Ohtani, H. *Coord. Chem. Rev.* **1985**, *64*, 1.

(3) Church, S. P.; Hermann, H.; Grevels, F.; Schaffner, K. *J. Chem. Soc. Chem. Commun.* **1984**, 785 and references therein.

(4) Freedman, A.; Bersohn, R. *J. Am. Chem. Soc.* **1978**, *100*, 4116.

(5) Leopold, D. G.; Vaida, V. *J. Am. Chem. Soc.* **1984**, *106*, 3720.

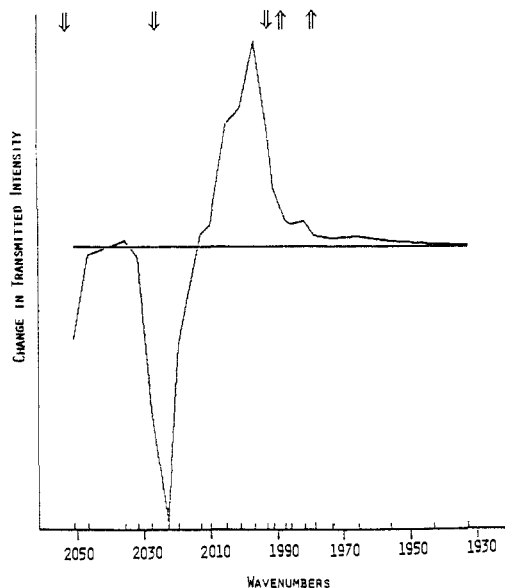


**Figure 1.** Transient infrared absorption spectrum obtained 25  $\mu$ s following XeF laser photolysis of gas-phase  $\text{Mn}_2(\text{CO})_{10}$ . The positive feature at 2000  $\text{cm}^{-1}$  is attributed to an  $\text{Mn}(\text{CO})_5$  absorption. The negative features arise from photolytic depletion of  $\text{Mn}_2(\text{CO})_{10}$ . Infrared absorptions of gas-phase  $\text{Mn}_2(\text{CO})_{10}$  and matrix-isolated  $\text{Mn}(\text{CO})_5$  are denoted by down arrows and up arrows, respectively. The tick marks above the ordinate depict the probe frequencies used to construct the spectrum.

occurring in  $\text{Mn}_2(\text{CO})_{10}$  for 351-nm radiation.

The time-resolved IR apparatus used for monitoring photochemically generated metal carbonyl transients in the gas phase has been previously described in detail.<sup>6</sup> Briefly, an excimer laser operating on XeF (3 mJ/cm<sup>2</sup>) was used to photolyze  $\text{Mn}_2(\text{CO})_{10}$ . Photofragments were monitored via their attenuation of infrared radiation (CO laser), as measured by a high-speed InSb detector. Spectral data were obtained by having a computer join points corresponding to the amplitude of the transient signals at various frequencies for a given time delay following the photolysis pulse.

Kinetic data for  $\text{Mn}(\text{CO})_5$  recombination were obtained from transients at a given probe laser wavelength. In these experiments the source of  $\text{Mn}_2(\text{CO})_{10}$  was a small amount of solid placed on the bottom of the flow cell. This provided a pressure of  $\sim 2$  mtorr of  $\text{Mn}_2(\text{CO})_{10}$  at room temperature. If desired, the cell could be warmed to 50  $^\circ\text{C}$  to increase this pressure.

Figure 1 shows the IR spectrum obtained 25  $\mu$ s after photolysis of 2 mtorr of  $\text{Mn}_2(\text{CO})_{10}$  in the presence of 15 torr of Ar buffer at 21  $^\circ\text{C}$ . Depletion of  $\text{Mn}_2(\text{CO})_{10}$  is evident at  $\sim 2023$   $\text{cm}^{-1}$ , illustrating that net photolysis has occurred. The positive absorption at  $\sim 2000$   $\text{cm}^{-1}$  is assigned to the  $\text{Mn}(\text{CO})_5$  radical. The assignment is based on correlation with known absorptions of solution-phase  $\text{Mn}(\text{CO})_5$  (1988  $\text{cm}^{-1}$ )<sup>3</sup> and the matrix-isolated species (1987.6 and 1978.4  $\text{cm}^{-1}$ ).<sup>7</sup> The observed difference in frequency between the gas-phase and condensed-phase bands for  $\text{Mn}(\text{CO})_5$  is compatible with the characteristic condensed-phase red shifting of infrared absorptions.

From studies involving the <sup>13</sup>CO substituted species, it has been shown that  $\text{Mn}(\text{CO})_5$  adopts the predicted<sup>8</sup>  $C_{4v}$  geometry in the matrix.<sup>7</sup> The E and A<sub>1</sub> bands of the matrix-trapped species were not resolved in solution<sup>3</sup> and, similarly, we have not been able to resolve these bands in the gas phase. Resolution of these bands is made more difficult by the convolution of the  $\text{Mn}(\text{CO})_5$  absorption with a parent band at 1993  $\text{cm}^{-1}$ . This parent band, which is easily seen in the gas-phase IR of  $\text{Mn}_2(\text{CO})_{10}$ , is not observable as a negative feature in Figure 1 due to an overlap with the intense

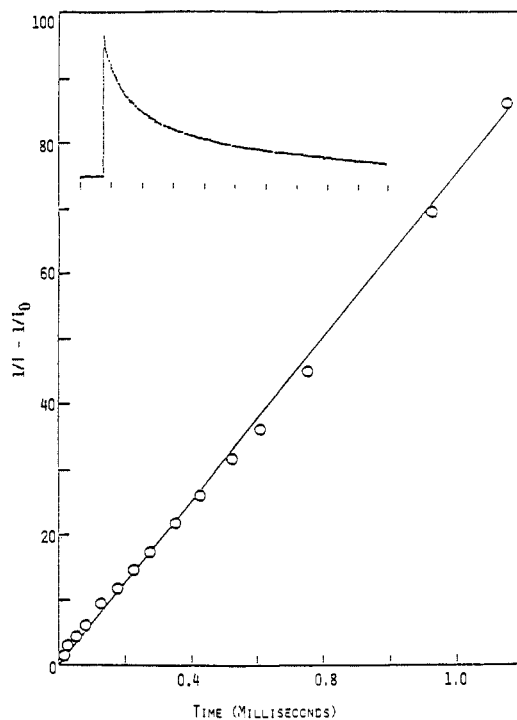
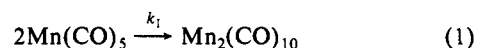


**Figure 2.** Disappearance of  $\text{Mn}(\text{CO})_5$  presented as a second-order decay. The data displayed in this figure were obtained from the transient absorption of  $\text{Mn}(\text{CO})_5$  at 2004.3  $\text{cm}^{-1}$ . The transient waveform, which is shown over a 2-ms range (inset), was obtained under the conditions described in the text, except that the cell temperature was 50  $^\circ\text{C}$ . From the slope of the curve,  $1/I$  measurements, and an estimated extinction coefficient, the rate constant for the second-order decay of  $\text{Mn}(\text{CO})_5$  is calculated to be  $(2.7 \pm 0.6) \times 10^{13}$   $\text{cm}^3 \text{mol}^{-1} \text{s}^{-1}$ . The value of  $\epsilon$  used in this calculation is that of  $\text{Mn}(\text{CO})_5\text{Cl}$  at 1988  $\text{cm}^{-1}$  ( $10^7$   $\text{cm}^2 \text{mol}^{-1}$ ). The error brackets represent the 95% confidence limits of the experimental data and do not account for the error introduced upon assuming a value for  $\epsilon$ .

$\text{Mn}(\text{CO})_5$  absorptions. Our assignment implies that gas-phase  $\text{Mn}(\text{CO})_5$  also is likely to have a  $C_{4v}$  geometry.

Identification of  $\text{Mn}(\text{CO})_5$  was confirmed by its kinetic behavior. Figure 2 shows a plot of the decay of the  $\text{Mn}(\text{CO})_5$  signal vs. time. The decay clearly follows a second-order rate law consistent with the reaction



Also,  $\text{Mn}_2(\text{CO})_{10}$  is seen to be regenerated as  $\text{Mn}(\text{CO})_5$  is depleted. As described in the caption of Figure 2, a rate constant of  $2.7 \times 10^{13}$   $\text{cm}^3 \text{mol}^{-1} \text{s}^{-1}$  can be determined from the data. Though the dependence of  $k_1$  on the buffer gas pressure has not been studied in detail, we have measured the same  $k_1$  at various buffer gas pressures. An estimate of the lifetime of  $\text{Mn}_2(\text{CO})_{10}$  formed via radical recombination confirms that third-body effects should be unimportant under our experimental conditions. This rate constant is quite close to that expected for a gas kinetic radical-radical recombination process, which is calculated to be  $\sim 1 \times 10^{14}$   $\text{cm}^3 \text{mol}^{-1} \text{s}^{-1}$ . This result is consistent with liquid-phase kinetic measurements, in which nearly diffusion-controlled rates have been observed for reaction 1.<sup>3</sup>

Interestingly, all of the initially photolyzed  $\text{Mn}_2(\text{CO})_{10}$  is not regenerated via reaction of  $\text{Mn}(\text{CO})_5$ . Moreover, though  $\text{Mn}(\text{CO})_5$  is inert to CO, addition of CO does lead to an increase in both the rate of regeneration and amount of  $\text{Mn}_2(\text{CO})_{10}$  regenerated. This is compatible with the regeneration of parent via reaction of CO with a photoproduct of  $\text{Mn}_2(\text{CO})_{10}$  which was produced via CO loss. By analogy with solution-phase studies, the simplest of these species is  $\text{Mn}_2(\text{CO})_9$ , though other species which have lost one or more COs are also possible. Thus we are presently working to verify whether  $\text{Mn}_2(\text{CO})_9$  can be detected via its characteristic semibridging CO absorption in the 1750- $\text{cm}^{-1}$  region. We are also investigating the possible production of other

(6) Ouderkirk, A. J.; Wermer, P.; Schultz, N. L.; Weitz, E. *J. Am. Chem. Soc.* **1983**, *105*, 3354.

(7) Church, S. P.; Poliakoff, M.; Timney, J. A.; Turner, J. J. *J. Am. Chem. Soc.* **1981**, *103*, 7515.

(8) Burdett, J. K. *J. Chem. Soc., Faraday Trans. 2* **1974**, *70*, 1599.

photoproducts that have lost one or more CO ligands, such as  $\text{Mn}(\text{CO})_x$  ( $x < 5$ ) and  $\text{Mn}_2(\text{CO})_y$  ( $y < 9$ ).

**Acknowledgment.** We thank the Air Force Office of Scientific Research for support of this work under Contract 83-0372. We also acknowledge support of this work by the donors of the Petroleum Research Fund, administered by the American Chemical Society. We thank Dr. Martyn Poliakoff and Prof. J. J. Turner for some very useful and informative discussions and are grateful for support from NATO, which facilitated these discussions.

Registry No.  $\text{Mn}_2(\text{CO})_{10}$ , 10170-69-1;  $\text{Mn}(\text{CO})_5$ , 15651-51-1.

## Heats of Formation and Homolytic Bond Dissociation Energies in the Keto-Enol Tautomers $\text{C}_2\text{H}_4\text{O}$ , $\text{C}_3\text{H}_6\text{O}$

John L. Holmes\* and F. P. Lossing

Chemistry Department, University of Ottawa  
Ottawa, Ontario, Canada K1N 9B4

Johan K. Terlouw

Analytical Chemistry Laboratory, University of Utrecht  
3522 AD Utrecht, The Netherlands

Received October 7, 1985

The measurement of appearance energies (AE) for ionic fragments whose heats of formation ( $\Delta H_f$ ) are well-known can lead to accurate  $\Delta H_f$  values for the neutral product of the dissociative ionization. Work in this laboratory has yielded  $\Delta H_f$  for the enol forms of acetaldehyde and acetone<sup>1</sup> and a number of simple organic free radicals.<sup>2</sup> The structure of the neutral product of an ion fragmentation for which a metastable peak is observed can be assigned via its collision-induced dissociative ionization (CIDI) mass spectrum. The latter can be obtained by the use of a double-focusing mass spectrometer of reversed geometry (e.g., V.G. Analytical ZAB-2F) which has been slightly modified<sup>3</sup> to permit only neutral fragmentation products to enter the collision cell<sup>4-6</sup> situated in the second field free region of the instrument.

We report here measurements of  $\Delta H_f$  for the radicals  $\dot{\text{C}}\text{H}_2\text{CHO}$  and  $\dot{\text{C}}\text{H}_2\text{COCH}_3$  and have derived the homolytic bond dissociation energies (HBDE)  $D[\text{H}-\dot{\text{C}}\text{H}_2\text{CHO}]$ ,  $D[\text{H}-\text{O}\dot{\text{C}}\text{HCH}_2]$ ,  $D[\text{H}-\dot{\text{C}}\text{H}_2\text{COCH}_3]$ , and  $D[\text{H}-\text{O}\dot{\text{C}}(\text{CH}_3)=\text{CH}_2]$ . The latter measurement yields a  $\Delta H_f$  value substantially different from that derived from gas-phase kinetic studies<sup>7</sup> and the associated HBDE is now in close agreement with the correlation between HBDE values and the barriers to internal rotation in the radicals described by Nonhebel and Walton.<sup>8</sup>

The compound  $\text{CH}_3\text{COOCHCH}_2$  has  $m/z$  43 as base peak in its normal mass spectrum. The reaction  $[\text{C}_4\text{H}_6\text{O}_2]^+ \rightarrow \text{C}_2\text{H}_3\text{O}^+ + \text{C}_2\text{H}_3\text{O}$  is accompanied by an intense, narrow Gaussian-type metastable peak. The fragment ions  $m/z$  43 have the structure  $[\text{CH}_3\text{C}^+\text{O}]$  as was shown by measuring their collisional activation mass spectrum and comparing it with that for acetyl ions.<sup>9</sup> Since the above metastable peak is the only one present in the ion kinetic

energy spectrum of  $[\text{CH}_3\text{COOCHCH}_2]^+$ , the structure of the neutral  $\text{C}_2\text{H}_3\text{O}$  species could be examined by its CIDI mass spectrum. Experimental details have been described elsewhere,<sup>3</sup> but in brief, the mass selected  $[\text{C}_4\text{H}_6\text{O}_2]^+$  ( $m/z$  86) ions fragment unimolecularly in the linear second field free region of the ZAB-2F spectrometer. All ions are deflected away and the high velocity (kV) neutral fragments pass into a cell containing a gas (He) where they are ionized by collision and subsequently fragment. Mass analysis of the ions is performed by the electric sector which is placed after the cell. It was observed that the CIDI mass spectrum of the  $\text{C}_2\text{H}_3\text{O}$  radicals was very closely similar to the charge reversal mass spectrum of  $\dot{\text{C}}\text{H}_2\text{CHO}$  anions,<sup>10</sup> showing that the radicals generated at energies near the dissociation threshold for  $[\text{CH}_3\text{COOCHCH}_2]^+$  were  $\dot{\text{C}}\text{H}_2\text{CHO}$ . Accordingly we have measured the AE  $m/z$  43 using energy-selected electrons.<sup>11</sup> The result,  $\text{AE} = 10.04 \pm 0.05$  eV, combined with  $\Delta H_f[\text{CH}_3\text{C}^+\text{O}] = 156 \pm 1$  kcal mol<sup>-1</sup><sup>12</sup> and  $\Delta H_f[\text{CH}_3\text{COOCHCH}_2] = -75.3 \pm 0.1$  kcal mol<sup>-1</sup><sup>13</sup> gives  $\Delta H_f[\dot{\text{C}}\text{H}_2\text{CHO}] = +0.2 \pm 2$  kcal mol<sup>-1</sup>. This  $\Delta H_f$  for the radical is in fair agreement with the  $3 \pm 2$  kcal mol<sup>-1</sup> derived from gas kinetics experiments by Rossi and Golden.<sup>14</sup> The HBDE from the present value is  $D[\text{H}-\dot{\text{C}}\text{H}_2\text{CHO}] = 92 \pm 2$  kcal mol<sup>-1</sup>. The strength of this bond can be compared with  $D[\text{H}-\dot{\text{C}}\text{H}_2\text{CHCH}_2]$  ( $86 \pm 1$  kcal mol<sup>-1</sup>).<sup>7</sup> An O-H bond strength can also be obtained. With  $\Delta H_f[\text{CH}_2\text{CHOH}] = -30$  kcal mol<sup>-1</sup>,<sup>1</sup> the value  $D[\text{H}-\text{O}\dot{\text{C}}\text{HCH}_2]$  in vinyl alcohol is  $82 \pm 2$  kcal mol<sup>-1</sup>, somewhat less than the corresponding bond strength in phenol,  $86.5 \pm 2$  kcal mol<sup>-1</sup>.<sup>7</sup>

Similar experiments were performed on the compounds  $\text{CH}_3\text{COOC}(\text{CH}_3)=\text{CH}_2$  and  $\text{CH}_3\text{COCH}_2\text{COCH}_3$ ; AE  $m/z$  43 was measured in each case and its structure confirmed to be  $[\text{CH}_3\text{C}^+\text{O}]$ ; the CIDI mass spectra of the neutral fragments were the same as that of charge-reversed  $\dot{\text{C}}\text{H}_2\text{COCH}_3$  anions.<sup>10</sup> AE  $m/z$  43 from  $\text{CH}_3\text{COOC}(\text{CH}_3)=\text{CH}_2$  ( $\Delta H_f = -84.1$  kcal mol<sup>-1</sup>, by additivity<sup>15</sup>) was  $9.88 \pm 0.05$  eV and from  $\text{CH}_3\text{COCH}_2\text{COCH}_3$  ( $\Delta H_f = -90.8$  kcal mol<sup>-1</sup>, by additivity<sup>15</sup>) was  $10.20 \pm 0.05$  eV, giving values for  $\Delta H_f[\dot{\text{C}}\text{H}_2\text{COCH}_3]$  of  $-12.3$  and  $-11.6 \pm 1$  kcal mol<sup>-1</sup>, respectively. It should be noted that AE values give upper rather than lower limits for the heats of formation of reaction products; however, the narrow metastable peaks accompanying the above fragmentations attest to the lack of either a significant kinetic shift or reverse energy barrier and so the observed AE values will be close to the reaction's thermochemical threshold.<sup>16</sup> Note that the effect of  $\text{CH}_3$  substitution in these radicals ( $-12$  kcal mol<sup>-1</sup>) is the same as the difference in heat of formation of an aldehyde and its corresponding methyl ketone.<sup>13,15</sup> The mean value for  $\Delta H_f[\dot{\text{C}}\text{H}_2\text{COCH}_3]$ ,  $-12 \pm 1.5$  kcal mol<sup>-1</sup>, is in poor agreement with the value of  $-5.7 \pm 1.8$  kcal mol<sup>-1</sup> selected in the recent review by McMillen and Golden.<sup>7</sup> However, we suggest that the latter value may be too high. Two HBDE values can be calculated from the new result, namely:  $D[\text{H}-\dot{\text{C}}\text{H}_2\text{COCH}_3] = 92 \pm 1.5$  kcal mol<sup>-1</sup> ( $\Delta H_f[\text{CH}_3\text{COCH}_3] = -51.9$  kcal mol<sup>-1</sup><sup>13</sup>) and  $78 \pm 2.5$  kcal mol<sup>-1</sup> for the O-H bond in the enol of acetone, for which  $\Delta H_f = -38 \pm 1$  kcal mol<sup>-1</sup>.<sup>1</sup>

Recently, Nonhebel and Walton<sup>8</sup> showed that a good linear relationship exists between the barriers to rotation in radicals  $[\text{R}-\dot{\text{C}}\text{H}_2]$  and the HBDE  $D[\text{H}-\dot{\text{C}}\text{H}_2\text{R}]$ . The magnitude of the barrier increases as the odd electron becomes more delocalized in the radical. The radical  $\dot{\text{C}}\text{H}_2\text{COCH}_3$  was anomalous, not lying on the line when its heat of formation was taken to be  $-6$  kcal mol<sup>-1</sup>, i.e.,  $D[\text{H}-\dot{\text{C}}\text{H}_2\text{COCH}_3] = 98$  kcal mol<sup>-1</sup>. We have replotted their line in Figure 1 using the present value for  $\dot{\text{C}}\text{H}_2\text{COCH}_3$  and

(1) Holmes, J. L.; Lossing, F. P. *J. Am. Chem. Soc.* **1982**, *104*, 2648.  
(2) Holmes, J. L.; Lossing, F. P. *Int. J. Mass. Spectrom. Ion Processes* **1984**, *58*, 113.  
(3) Holmes, J. L.; Mommers, A. A. *Org. Mass Spectrom.* **1984**, *19*, 460.  
(4) Burgers, P. C.; Holmes, J. L.; Mommers, A. A.; Terlouw, J. K. *Chem. Phys. Lett.* **1983**, *102*, 1.  
(5) Burgers, P. C.; Holmes, J. L.; Mommers, A. A.; Szulejko, J. E.; Terlouw, J. K. *Org. Mass Spectrom.* **1984**, *19*, 442.  
(6) Clair, R.; Holmes, J. L.; Mommers, A. A.; Burgers, P. C. *Org. Mass Spectrom.* **1985**, *20*, 207.  
(7) McMillen, D. F.; Golden, D. M. *Annu. Rev. Phys. Chem.* **1982**, *33*, 493.  
(8) Nonhebel, D. C.; Walton, A. C. *J. Chem. Soc., Chem. Commun.* **1984**, 731.  
(9) Burgers, P. C.; Holmes, J. L.; Szulejko, J. E.; Mommers, A. A.; Terlouw, J. K. *Org. Mass Spectrom.* **1983**, *18*, 254.

(10) Lehman, T. A.; Bursley, M. M.; Hass, J. R. *Org. Mass Spectrom.* **1983**, *18*, 373.  
(11) Lossing, F. P.; Traeger, J. C. *Int. J. Mass Spectrom. Ion Phys.* **1976**, *19*, 9.  
(12) Traeger, J. C.; McLoughlin, R. G.; Nicholson, A. J. C. *J. Am. Chem. Soc.* **1982**, *104*, 5318.  
(13) Pedley, J. B.; Rylance, J. "Computer Analysed Thermochemical Data: Organic and Organometallic Compounds"; University of Sussex, 1977.  
(14) Rossi, M.; Golden, D. M. *Int. J. Chem. Kinet.* **1979**, *11*, 715.  
(15) By additivity: Benson, S. W. "Thermochemical Kinetics"; Wiley Interscience: New York, 1976.  
(16) Holmes, J. L. *Org. Mass Spectrom.* **1985**, *20*, 169.